Ca^{2+}- and H^+-Dependent Conformational Changes of Calbindin D_{28k}[†]

Tord Berggård,[‡] Maria Silow,[§] Eva Thulin,[‡] and Sara Linse*,[‡]

Physical Chemistry 2 and Department of Biochemistry, Chemical Centre, University of Lund, S-221 00 Lund, Sweden

Received October 14, 1999; Revised Manuscript Received March 14, 2000

ABSTRACT: Calbindin D_{28k} is a member of a large family of intracellular Ca^{2+} binding proteins characterized by EF-hand structural motifs. Some of these proteins are classified as Ca^{2+}-sensor proteins, since they are involved in transducing intracellular Ca^{2+} signals by exposing a hydrophobic patch on the protein surface in response to Ca^{2+} binding. The hydrophobic patch serves as an interaction site for target enzymes. Other members of this group are classified as Ca^{2+}-buffering proteins, because they remain closed after Ca^{2+} binding and participate in Ca^{2+} buffering and transport functions. ANS (8-anilinonaphthalene-1-sulfonic acid) binding and affinity chromatography on a hydrophobic column suggested that both the Ca^{2+}-free and Ca^{2+}-loaded form of calbindin D_{28k} have exposed hydrophobic surfaces. Since exposure of hydrophobic surface is unfavorable in the aqueous intracellular milieu, calbindin D_{28k} most likely interacts with other cellular components in vivo. A Ca^{2+}-induced conformational change was readily detected by several optical spectroscopic methods. Thus, calbindin D_{28k} shares some of the properties of Ca^{2+}-sensor proteins. However, the Ca^{2+}-induced change in exposed hydrophobic surface was considerably less pronounced than that in calmodulin. The data also shows that calbindin D_{28k} undergoes a rapid and reversible conformational change in response to a H^+ concentration increase within the physiological pH range. The pH-dependent conformational change was shown to reside mainly in EF-hands 1−3. Urea-induced unfolding of the protein at pH 6, 7, and 8 showed that the stability of calbindin D_{28k} was increased in response to H^+ in the range examined. The results suggest that calbindin D_{28k} may interact with targets in a Ca^{2+}- and H^+-dependent manner.

The calmodulin superfamily contains proteins with high affinities for Ca^{2+}. Well-known members of this family are calmodulin, troponin C, calcineurin, and the S-100 proteins. A common structural feature is the so-called EF-hand motif (*1*), which adopts a helix−loop−helix conformation and has the ability to bind one calcium ion. The calcium ion is coordinated by oxygen atoms provided by carboxylate side chains, backbone amide carbonyls, and water molecules. The majority of the proteins within the superfamily contain 2−4 EF-hands and bind Ca^{2+} with positive cooperativity. The domain organization varies considerably between different EF-hand proteins. Although small EF-hand-pair domains are seen in many cases, there are several examples of larger domains containing more than two EF-hands (for a review, see ref *2*).

Calbindin D_{28k} is a highly conserved member of the calmodulin superfamily. This six-EF-hand protein was first found in avian intestine (*3*), and then also in other tissues including kidney and pancreas (*4*, *5*). During later years this protein has attracted much attention due to its abundance in specific neuronal cell types in the central nervous system (*6*−*12*). In fact, calbindin D_{28k} constitutes between 0.1% and 1.5% of the total soluble protein in brain (*13*). It is highly homologous to calretinin, another six-EF-hand protein, which is also abundant in a subpopulation of brain neurons.

Calbindin D_{28k} has a high affinity for Ca^{2+} [$K_a = 10^6$−10^7 M^{-1} in 150 mM KCl (*14*) and 10^8 M^{-1} at low ionic strength (*15*)]. The stoichiometry of Ca^{2+} binding is controversial. The reported number of high-affinity sites is 3 (*16*), 3−4 (*17*), 4 (*14*, *18*), or 5−6 (*15*). A study with synthetic EF-hand peptides identified four regular EF-hand sites and a fifth site in a noncanonical EF-hand (*19*).

Many functions of calbindin D_{28k} have been proposed on the basis of the hypothesis that the protein acts as an endogenous calcium buffer. It is of importance for motor coordination in mice (*20*) and has been suggested to restrict evoked Ca^{2+} signals in nerve synapses and hair cells by acting as a mobile calcium buffer (*21*, *22*). Calbindin D_{28k} has been demonstrated to protect against excitotoxic cell death in hippocampal neurons (*23*), and other studies have reported selective survival of neurons containing calbindin D_{28k} following ischemic insults or seizures, where damage is believed to occur via Ca^{2+}-mediated excitotoxicity (*24*, *25*). The protein has also been proposed to facilitate the diffusional flux of Ca^{2+} in the intestinal enterocyte (*26*).

EF-hand proteins that interact directly with and modulate the activity of other proteins in a Ca^{2+}-dependent manner are often termed Ca^{2+}-sensor proteins, whereas those involved in Ca^{2+}-buffering and transport functions are termed Ca^{2+}-buffer proteins (for a review see ref *27*). A typical Ca^{2+} sensor, like calmodulin, undergoes large structural rearrangements upon binding of Ca^{2+}, resulting in exposure of

[†] This work was supported with grants from the Swedish Natural Science Research Foundation (NFR K-Ku.10178-300, S.L.) and from a postdoctoral stipend from Salubrin/Druvan AB (T.B.).

* Correspondence should be addressed to this author. Telephone +46-46-2228246; fax +46-46-2224543; email Sara.Linse@fkem2.lth.se.

[‡] Physical Chemistry 2.

[§] Department of Biochemistry.

10.1021/bi992394g CCC: $19.00
Published on Web 05/12/2000

hydrophobic surfaces, which are essential for interaction with target proteins. In contrast, a Ca^{2+}-buffer/transport protein like calbindin D_{9k} remains closed after Ca^{2+} binding (*28*). On the basis of the functional studies and the apparent absence of cellular targets, calbindin D_{28k} is often classified solely as a Ca^{2+}-buffering protein. In this work, a biophysical characterization of calbindin D_{28k} from three species was undertaken in order to investigate possible sensor functions of the protein.

EXPERIMENTAL PROCEDURES

Proteins. Human calbindin D_{28k} was expressed in *Escherichia coli* and purified to homogeneity as described (*29*). The purification of chicken intestinal calbindin D_{28k} was accomplished by the method of Friedlander and Norman (*30*). Bovine brain calbindin D_{28k} was purified as follows. Four bovine brains were taken 0−1 h postmortem, yielding 1.020 kg of brain tissue, which was homogenized in 1.2 L of buffer A (10 mM MES,[1] 1 mM DTT, 4 mM EDTA, pH 5.6). The slurry was centrifuged for 20 min at 10 000 rpm. The pellet was again homogenized in 1.2 L of buffer A and centrifuged. The supernatants from both spins were slammed with a total of approximately 350 mL of DEAE-cellulose (ion-exchange resin)[2] and the cellulose was collected on a Büchner funnel. The DEAE-cellulose was then washed with buffer A and packed in a 5.5 × 15 cm column. Proteins were eluted with a 1.0 L linear salt gradient from 0 to 0.4 M NaCl in buffer A. Fractions between 0.2 and 0.3 M NaCl were pooled because they displayed a band that comigrated with human recombinant calbindin D_{28k} in agarose gel electrophoresis and was recognized by a monoclonal antibody against calbindin D_{28k} (Swant, Bellinzona, Switzerland). The fractions were diluted with 210 mL of H_2O, adjusted to 2 mM DTT and 1 mM $CaCl_2$, and pumped onto a 3.4 × 12 cm DEAE-Sephacel ion-exchange column equilibrated in buffer B (10 mM MES, 1 mM DTT, and 2 mM $CaCl_2$, pH 5.6). Proteins were eluted by a linear salt gradient from 0 to 0.4 M NaCl in buffer B. The pooled fractions were freeze-dried and separated on a Sephadex G50 superfine size-exclusion column (3.4 × 180 cm) in 50 mM NH_4Ac, pH 6.0. Fractions with calbindin D_{28k} immunoreactivity were pooled, supplemented with 1 mM EDTA, and pumped on a 1.5 × 9 cm DEAE-Sephacel ion-exchange column. The column was washed with 50 mL of buffer A and eluted with a 600 mL linear gradient of 0−0.3 M NaCl. After this procedure, the pooled fractions were free from other proteins, and were lyophilized and desalted on a Sephadex G25 superfine gel-filtration column.

The purity of each protein was assessed by agarose gel electrophoresis in the presence of 1 mM EDTA or 2 mM calcium lactate, SDS−PAGE, immunoblotting, isoelectric focusing, and mass spectrometry. All three proteins were detected by the commercial monoclonal antibody against calbindin D_{28k} (Swant) and all three had the same mobility in SDS−PAGE, which was in agreement with the molecular mass of close to 30 kDa. Agarose gel electrophoresis and isoelectric focusing showed that the purified proteins were free from deamidated material. The human and bovine proteins had the same mobility in agarose gel electrophoresis, while the chicken protein had a slightly higher mobility as expected from the sequence differences, which predict one unit higher net negative charge on the chicken protein. The three proteins exhibited an identical shift in mobility upon comparison of gels in calcium and EDTA.

Two fragments, comprising EF-hands 1−3 and 4−6, respectively, were expressed in *E. coli* from truncated genes and purified in 10 mM MES, pH 5.6, as described for human calbindin D_{28k} (*29*), by the following steps: (1) heat precipitation of bacterial proteins, (2) DEAE-cellulose anion-exchange chromatography in 10 mM MES buffer at pH 5.6 with 1 mM $CaCl_2$, (3) DEAE-Sephacel anion-exchange chromatography in 10 mM MES buffer at pH 5.6 with 1 mM EDTA, and (4) dialysis against doubly distilled water to remove buffer and NaCl. The procedure will be described in detail elsewhere (Berggård et al., manuscript in preparation). The purity was confirmed by the same methods as for intact calbindin D_{28k}. Bovine calmodulin was expressed in *E. coli* and purified by ion-exchange chromatography, followed by gel filtration and affinity chromatography as described (*31*). Bovine calbindin D_{9k} was expressed in *E. coli* and purified as described (*32*).

To produce Ca^{2+}-free proteins, purified protein was dissolved in 1 mL of doubly distilled water containing a 10−20-fold excess of EGTA at pH 8. The sample was applied to a 3.4 × 20 cm Sephadex G25 superfine gel-filtration column. To abolish EGTA binding, the protein was applied to the column after 15 mL of saturated NaCl had been allowed to penetrate the top of the column. The NaCl solution had been depleted from residual Ca^{2+} by dialysis against Chelex-100 resin. During the gel filtration, the protein passed through the NaCl zone and was eluted free from EGTA in doubly distilled Ca^{2+}-free water. ^1H NMR spectra confirmed that the proteins were free from EGTA and buffer salts. The residual calcium content after the calcium depletion was between 0.2 and 0.6 equiv as measured by quin 2-based assays.

Urea Denaturation. A 133 μM stock of calbindin D_{28k} was prepared by dissolving 6.55 mg of lyophilized apo calbindin D_{28k} in 1350 μL of 1 mM DTT, 10 mM KH_2PO_4, and 0.5 mM EGTA, pH 7.0. A 10 M stock solution of urea was prepared by adding 6.006 g of ultrapure urea to 3333 μL of 30 mM KH_2PO_4, and 1.5 mM EGTA, pH 7.0, and adjusting the pH to the desired value and the volume to 10 mL with H_2O. Buffer (10 mM KH_2PO_4 and 0.5 mM EGTA, pH adjusted to the desired value) and urea stock solution were then mixed in varying proportions to give samples with urea concentrations ranging from 0 to 9.7 M. The samples contained a constant amount (30 μL) of the calbindin D_{28k} stock to give a final protein concentration of 8 μM of calbindin D_{28k} in all samples. The ellipticity at 222 nm and the intrinsic (tryptophan) fluorescence emission at 354 nm (excitation at 295 nm) were measured, after subtraction of background buffer spectra, at 25 °C on a Jasco-720 spectropolarimeter or a Perkin-Elmer luminescence spectrometer LS 50 B connected to a Julabo F25 thermostatic water bath. In the CD experiments, a 1 mm quartz cuvette was used.

[1] Abbreviations: PBS, phosphate-buffered saline; ANS, 8-anilinonaphthalene-1-sulfonic acid, ammonium salt; EDTA, ethylendinitrilotetraacetic acid, disodium salt, dihydrate; CD, circular dichroism; SDS, sodium dodecyl sulfate; PAGE, polyacrylamide gel electrophoresis; MES, 2-(*N*-morpholino)ethanesulfonic acid; DTT, dithiothreitol; BSA, bovine serum albumin.

[2] We noted that the amount of DEAE-cellulose used was not sufficient to bind all calbindin D_{28k}.

The experiments were analyzed with KaleidaGraph software (Synergy Software) for Macintosh and fitted to a linear extrapolation model with two-state unfolding assumed (*33*). The baselines before, Y_N, and after, Y_U, the actual unfolding, were assumed to be straight lines:

$$Y_N = k_N[D] + b_N \quad (1)$$

$$Y_U = k_U[D] + b_U \quad (2)$$

where k_N and k_U are the slopes, b_N and b_U are intercepts, and [D] is the denaturant concentration. Y_N and Y_U hence correspond to the ellipticity of the native and unfolded state, respectively, as a function of urea concentration. The observed ellipticity or fluorescence emission at 354 nm, Y_o, was fitted with

$$Y_o = \frac{(k_N[D] + b_N) + (k_U[D] + b_U)e^{-(\Delta G_{NU}(H_2O) - m_D[D])/RT}}{1 + e^{-(\Delta G_{NU}(H_2O) - m_D[D])/RT}} \quad (3)$$

where $\Delta G_{NU}(H_2O)$ is the unfolding free energy in pure water, m_D is the influence of denaturation concentration on the stability, R is the molar gas constant, and T is the temperature. The free energy toward unfolding by urea, ΔG_{NU}, is assumed to obey the linear equation:

$$\Delta G_{NU} = \Delta G_{NU}(H_2O) - m_D[D] \quad (4)$$

C_m, the urea concentration at the transition midpoint, was calculated from eq 4 by setting ΔG_{NU} to zero. The errors in the reported values of the different parameters were estimated to one standard deviation. The standard deviations were obtained directly from the fitting procedures. For presentation, the data were normalized according to

$$F_{app} = (Y_O - Y_N)/(Y_U - Y_N) \quad (5)$$

and fitted to

$$F_{app} = \frac{e^{-(\Delta G_{NU}(H_2O) - m_D[D])/RT}}{1 + e^{-(\Delta G_{NU}(H_2O) - m_D[D])/RT}} \quad (6)$$

Spectroscopic Analyses. Structural differences between the apo and Ca^{2+}-loaded forms of calbindin D_{28k} were investigated by CD spectroscopy, UV absorbance analysis, and fluorescence spectroscopy. A stock of approximately 10 mg/mL calbindin D_{28k} in H_2O was prepared and an aliquot was withdrawn and subjected to acid hydrolysis to determine the protein concentration accurately. The stock was then used to prepare a protein solution (68 μM calbindin D_{28k}, 10 mM DTT, 0.125 mM EDTA, and 2 mM Tris, pH 6.5−8.0), which was used to record the intrinsic (tryptophan) fluorescence emission spectrum (excitation at 295 nm) and CD and UV spectra in the near-UV range (250−300 nm). The far-UV CD spectrum (185−250 nm) was measured at a lower protein concentration (9 μM). $CaCl_2$ (1.25 mM) was added to the protein solutions, and the same measurements were performed again to yield spectra for the Ca^{2+} form. UV absorbance measurements were recorded on a GBC UV/vis 920 spectrophotometer. CD spectra were obtained on a Jasco J-720 spectropolarimeter at 25 °C (thermostated). Fluorescence spectra were obtained on a Perkin-Elmer luminescence spectrometer LS 50 B connected to a Julabo F25 thermostatic water bath. All data were collected at 25.0 °C. Quartz cuvettes with path lengths of 10, 3, 1, or 0.1 mm were used.

ANS Fluorescence Measurements. To monitor the changes of the ANS emission spectra induced by difference in the concentration of salt and/or presence of Ca^{2+}, 2 mL of 12 μM of calbindin D_{28k} or calmodulin was prepared in either 1 mM DTT, 2 mM Tris, and 0.15 M KCl or 1mM DTT and 2 mM Tris in the presence of excess of either EDTA (50 μM) or $CaCl_2$ (100 μM). ANS fluorescence emission spectra were recorded between 400 and 600 nm with excitation at 385 nm. The excitation slit was 3 nm and the emission slit was 8 nm. The protein was saturated with 60 μM ANS. To monitor the effect of H^+ concentration, the pH was changed by titration with KOH or HCl. The excitation slit was 3 nm and the emission slit was 7 nm. In some experiments, recombinant fragments comprising EF-hands 1−3 or EF-hands 4−6 at a concentration of 3.6 μM in 1 mM DTT, 0.15 M KCl, 50 μM EDTA, and 30 μM ANS were used. The excitation slit was 3 nm and the emission slit was 10 nm. The pH value was measured on a Mettler-Toledo U402-M3-S7/200 pH electrode. For each experimental setting, ANS spectra for Ca^{2+}-free and Ca^{2+}-loaded calmodulin were recorded to enable a quantitative comparison of different forms.

Size Exclusion Chromatography. Determination of the multimerization status of calbindin D_{28k} was performed by size-exclusion chromatography on a Pharmacia Superdex 75 FPLC with a Bio-Rad Biologic HR Workstation system. The chromatography buffer was 50 mM MOPS, 150 mM NaCl, and 1 mM DTT in the presence of 1 mM $CaCl_2$ or 1 mM EDTA. The pH was adjusted to 6.5 or 7.9.

Binding of Calbindin D_{28k} to Phenyl Superose. Ca^{2+}-dependent hydrophobicity was analyzed by subjecting calmodulin, calbindin D_{9k}, or calbindin D_{28k} to chromatography on a hydrophobic column (phenyl-sepharose high-performance column from Amersham Pharmacia Biotech). The proteins were eluted with a reverse salt gradient from 1 M NaCl and 2 mM Tris, pH 7.1, containing 50 μM EDTA or 1 mM $CaCl_2$, to 2 mM Tris, pH 7.1. Prior to the injection, 10 μL of a stock solution (10 mg/mL) of the protein was dissolved in 200 μL of the high-salt buffer. The conductance and the absorbance at 214 nm were recorded.

RESULTS

Interaction of Calbindin D_{28k} with ANS: Comparison with Calmodulin and Calbindin D_{9k}. ANS has been widely used in monitoring exposed hydrophobic patches on the surface of proteins during folding and to monitor conformational changes. ANS fluorescence is strongly dependent on the polarity of the local environment around the chromophore. In water the emission is weak, with a maximum around 520 nm. Upon binding to hydrophobic patches of proteins, the fluorescence spectrum is blue-shifted with a maximum around 475 nm and the emission intensity is increased. The blue shift results from reduced solvent relaxation in a less polar environment and is a reliable reporter of the hydrophobicity around the bound ANS. The intensity increase is due to reduced solvent quenching and is a less reliable parameter as there are many other factors that may contribute to the fluorescence quenching, for example, protein dynamics

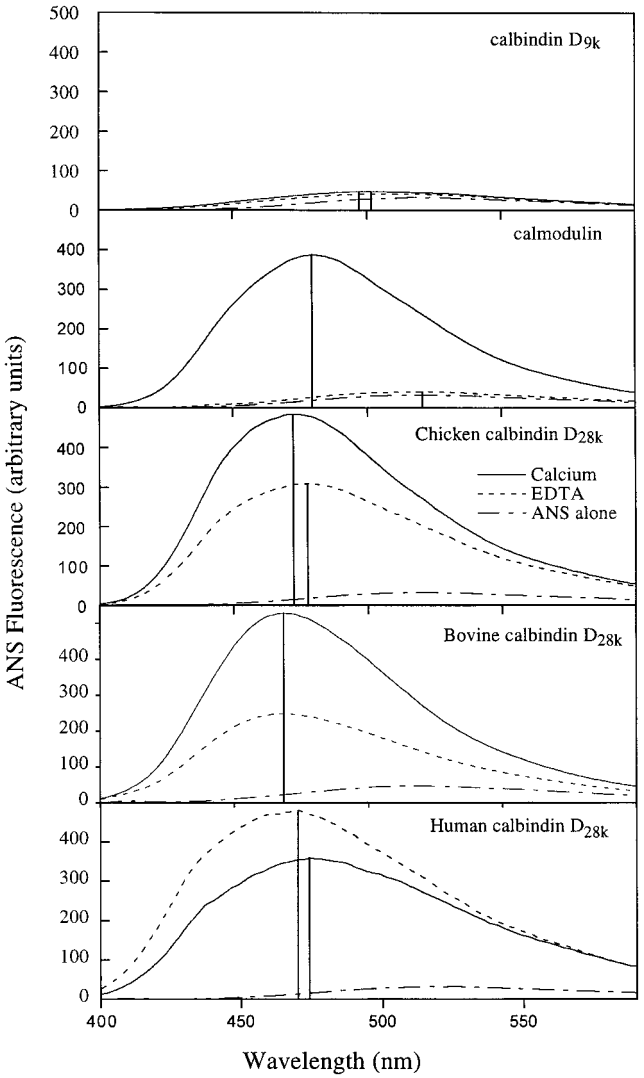

FIGURE 1: ANS binding to human, bovine, or chicken calbindin D_{28k} in comparison with calmodulin and calbindin D_{9k}. Human, bovine, or chicken calbindin D_{28k}, bovine calmodulin, or bovine calbindin D_{9k} was dissolved to 12 μM concentration in 2 mL of 60 μM ANS, 50 μM EDTA, 1 mM DTT, and 0.15 M KCl, pH 7.8. The ANS fluorescence emission spectra (excitation at 385 nm) were recorded at room temperature (Ca^{2+}-free forms; ---). $CaCl_2$ (1 μL 1M) was then added to each solution (Ca^{2+}-loaded forms; —) and the measurements were repeated. (— - —) Spectrum for 60 μM ANS in buffer without protein. The wavelength positions of fluorescence intensity maxima are shown as vertical bars.

and bound metal ions. Ca^{2+} effects on ANS fluorescence were studied for calbindin D_{28k} in parallel with a typical Ca^{2+} sensor, calmodulin, and a typical Ca^{2+} buffer, calbindin D_{9k} (Figure 1).

As expected, both the apo and Ca^{2+} forms of calbindin D_{9k} and the apo state of calmodulin showed only a negligible binding of ANS, whereas ANS bound strongly to Ca^{2+}-loaded calmodulin, which is seen as a significant blue shift (40 nm, from 520 to 480 nm) and an enhancement of the fluorescence. In striking contrast, the ANS fluorescence was significantly enhanced and blue-shifted (by 43−51 nm) for both the Ca^{2+}-free and Ca^{2+}-loaded forms of calbindin D_{28k}, Both forms caused a larger ANS blue shift than Ca^{2+}-loaded calmodulin, and this behavior was observed for human and bovine as well as chicken calbindin D_{28k}. There were small deviations in the wavelength maxima for the Ca^{2+} forms from

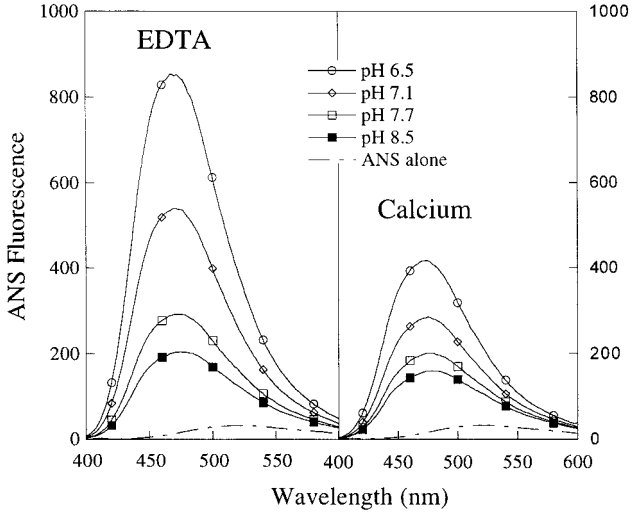

FIGURE 2: Effect of pH on the ANS binding to Ca^{2+}-free and Ca^{2+}-loaded calbindin D_{28k}. Fluorescence spectra of 60 μM ANS in the presence of 12 μM human recombinant calbindin D_{28k} in 1 mM DTT and 0.15 M KCl. Spectra were recorded at various pHs in the presence of 50 μM EDTA or 100 μM $CaCl_2$ as indicated in the figure (excitation at 385 nm). (— - —) Spectrum for 60 μM ANS in buffer without protein.

the three species (474 nm for human, 473 nm for chicken, and 469 nm for bovine calbindin D_{28k}) and a slightly larger spread for the apo forms (470 nm for human, 477 nm for chicken, and 469 nm for bovine calbindin D_{28k}). Hence, the Ca^{2+}-induced effect on ANS fluorescence was a slight red shift (4 nm) for human recombinant calbindin D_{28k}, a small blue shift (4 nm) for chicken calbindin D_{28k}, and no observable shift for the bovine protein. Despite these variations between the species, it is clear that calbindin D_{28k} does not behave as any of the two control proteins, calbindin D_{9k} and calmodulin, because the fluorescence of ANS is significantly enhanced and blue-shifted for both the apo and Ca^{2+} forms of calbindin D_{28k}.

Although fluorescence intensities are less reliable, due to the many factors that can lead to quenching, we noted that there are reproducible differences between the three proteins. For human calbindin D_{28k}, there is a higher intensity in the apo state, while for bovine and chicken calbindin D_{28k}, the highest intensity is found for the Ca^{2+} state. We also noted that low ionic strength (protein dissolved in 2 mM Tris instead of 2 mM Tris and 0.15 M KCl) reduces the ANS fluorescence of both the apo and Ca^{2+} forms of calbindin D_{28k} by a factor of approximately 2 (data not shown).

The enhancement of ANS fluorescence was markedly dependent on pH (Figure 2). Since the fluorescence of ANS alone is not dependent on pH in the range studied, the H^+-induced fluorescence enhancement in the presence of calbindin D_{28k} may be the result of an increased accessibility of surfaces with affinity for ANS at lower pH, or a pH-induced effect on the environment around the bound ANS. A stepwise change of the pH from pH 8.5 to 6.0 and back by addition of HCl or NaOH returned the ANS fluorescence to the initial value, indicating that the conformational shift induced by H^+ is rapid and reversible. As a control, ANS binding to calmodulin was studied at different pHs, but no significant difference was observed in the pH range of 6.5−8.5 (data not shown). Similar negative results have been reported for several other proteins, like myokinase, alkaline

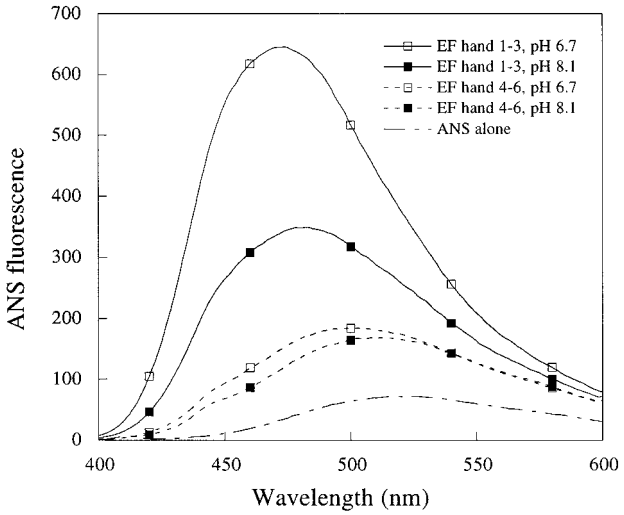

FIGURE 3: Effect of pH on the ANS binding to fragments of human calbindin D_{28k}. Fluorescence spectra of 30 μM ANS in the presence of 3.6 μM of a recombinant fragment comprising either EF hand 1−3 (—) or EF hand 4−6 (---) in 1mM DTT, 0.15 M KCl, and 50 μM EDTA at pH 6.7 and 8.1 as indicated in the figure (excitation at 385 nm). (− - −) Spectrum for 30 μM ANS in buffer without protein.

phosphatase, and acid phosphatase (*34*), suggesting that pH-dependent binding of hydrophobic probes to proteins in the pH range examined is uncommon.

At all pHs, the apo form of human recombinant calbindin D_{28k} produced more intense and more blue-shifted ANS spectra than the Ca^{2+}-loaded form. The difference in ANS spectra between the apo- and Ca^{2+}-loaded forms was more pronounced at lower pHs. Thus, the ratio of ANS fluorescence intensity at 470 nm of Ca^{2+}-loaded calbindin D_{28k} versus Ca^{2+}-free calbindin D_{28k} was 0.48 at pH 6.5, 0.53 at pH 7.1, 0.68 at pH 7.7, and 0.78 at pH 8.5. When the pH was decreased from 8.5 to 6.5, human recombinant calbindin D_{28k} displayed a blue shift in the fluorescence intensity maximum from 475 to 467 nm in the absence of Ca^{2+}, and from 479 to 470 nm in the presence of Ca^{2+}. This suggests that the local environment around the excited ANS molecules becomes less polar at lower pH. Bovine brain and chicken intestinal calbindin D_{28k} also displayed a blue shift and enhancement in ANS fluorescence intensity maximum when the pH was decreased (not shown). Like the human protein, the difference in the ANS emission maxima and intensities between the Ca^{2+} and apo form was highly dependent on pH. For example, the ratio of ANS fluorescence intensity at 470 nm of Ca^{2+}-loaded chicken calbindin D_{28k} versus Ca^{2+}-free protein was 1.6 at pH 8, whereas at pH 6.5, the ratio was only 1.1. A similar trend was seen for the bovine protein. Hence, the pH-induced structural changes detected by ANS binding are more pronounced in the Ca^{2+}-free protein.

A recombinant fragment of calbindin D_{28k} comprising EF-hand 1−3 (residues 1−132) showed an approximately 9-fold enhancement of ANS fluorescence (compared to ANS in buffer) with a maximum intensity at 474 nm at pH 6.7 (Figure 3). When the pH was raised to 8.1, the enhancement of ANS fluorescence intensity was reduced by a factor of 2 and the emission maximum was red-shifted to 483 nm. Contrary to this, a fragment comprising EF-hand 4−6 (residues 133−261) showed a comparatively low enhancement of ANS fluorescence and a maximum intensity at 501 nm at pH 6.7. When the pH was raised to 8.1, the wavelength maximum was red-shifted to 511 nm with only a very small reduction in maximum intensity. The results suggest that the structural elements responsible for the acid-induced ANS fluorescence enhancement reside mainly in the N-terminal half (residues 1−132) of calbindin D_{28k}. When recorded in parallel, the sum of the emission spectra for the two fragments was equal to the spectrum of the intact protein within experimental error (less than 5% deviation).

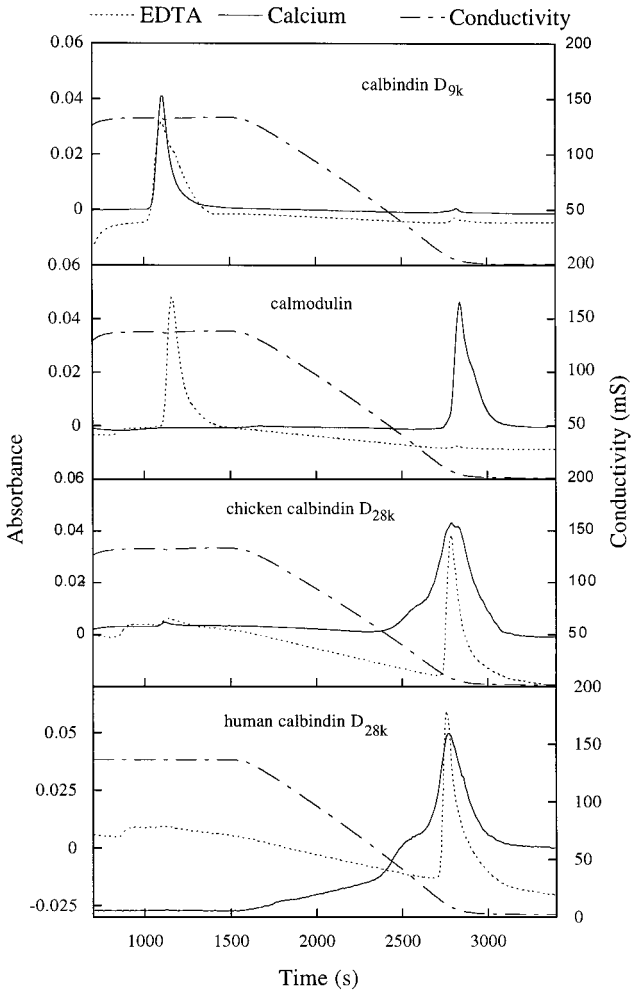

FIGURE 4: Hydrophobic chromatography for calmodulin, calbindin D_{9k}, and calbindin D_{28k}. Calbindin D_{9k} calmodulin, chicken calbindin D_{28k}, or human calbindin D_{28k} was applied onto a hydrophobic column (phenyl-Sepharose high-performance column from Amersham Pharmacia Biotech). Prior to the injection, 10 μL of a stock solution (10 mg/mL) of the protein was dissolved in 200 μL of the high salt buffer. The proteins were eluted with a decreasing salt gradient from 1 M NaCl and 2 mM Tris in 50 μM EDTA, pH 7.1 (Ca^{2+}-free forms; ---) or 1 mM $CaCl_2$ (Ca^{2+}-loaded forms; —) to 2 mM Tris, pH 7.1. The conductivity (− - −) and the absorbance at 214 nm were followed.

Binding of Calbindin D_{28k} to a Hydrophobic Resin. The ANS experiments indicate that calbindin D_{28k} has exposed hydrophobic surfaces in both the apo and Ca^{2+} forms. To verify this, calbindin D_{28k} was loaded on a phenyl-Superose column in the presence of 50 μM EDTA or 1 mM $CaCl_2$ and eluted with a decreasing salt gradient from 1 to 0.0 M NaCl. As controls, calbindin D_{9k} and calmodulin were included. Calbindin D_{9k} eluted very early in the gradient in both the presence and absence of Ca^{2+} (Figure 4). In contrast, calmodulin eluted early in the gradient in the absence of Ca^{2+}

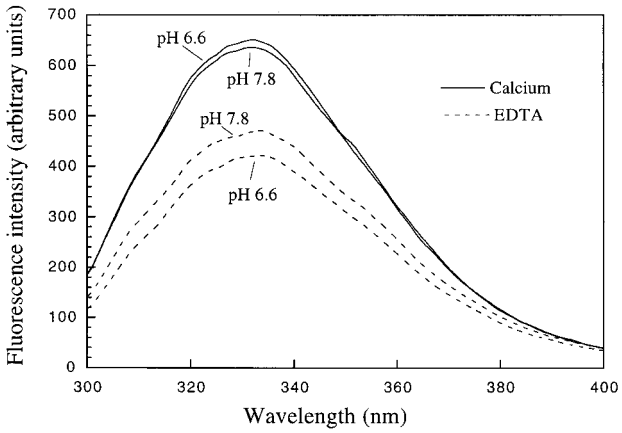

FIGURE 5: Tryptophan fluorescence spectra of Ca^{2+}-free and Ca^{2+}-loaded calbindin D_{28k}. The intrinsic (tryptophan) fluorescence emission spectrum (excitation at 295 nm) was recorded at 25 °C and pH 6.6 or 7.8 for a solution of 68 μM human recombinant calbindin D_{28k} in 10 mM DTT, 0.125 mM EDTA, and 2 mM Tris (apo calbindin D_{28k}; ---). $CaCl_2$ (1.25 mM) was then added to the same solution (Ca^{2+}-calbindin D_{28k}; —).

but late in the presence of Ca^{2+}. Calbindin D_{28k} from all three species eluted late in both the presence and absence of Ca^{2+}.

The data in Figure 4 were obtained in the absence of DTT, and the extra hump observed at ca. 2600 s for calbindin D_{28k} in Ca^{2+} was found to be disulfide-bonded dimers. Collected fractions were subjected to nonreducing SDS−PAGE, and fractions from the hump yielded a band at twice the M_w of calbindin D_{28k}, while the major peak at 2800 s contained protein with the monomer M_w. Initial experiments on the hydrophobic column were performed with DTT in the running buffer. Although these data were of poor quality due to the high background absorbance of DTT, runs in the absence and presence of Ca^{2+} yielded protein peaks at the same positions as the major peaks in Figure 4.

Size-Exclusion Chromatography. To establish a possible correlation between dimerization and exposure of hydrophobic groups, human recombinant calbindin D_{28k} was subjected to size-exclusion chromatography (not shown). The results suggest that, when reduced by DTT, the protein migrates as a monomer at both pH 7.9 and 6.5 in the presence or absence of Ca^{2+}. Thus, the pH-dependent conformational change does not reflect dimerization or multimerization of the protein. We noted, however, that the protein has a tendency to form disulfide-linked dimers in nonreduced samples. These complexes are most likely not physiologically relevant since the cytosol contains a high concentration of reducing agents that prevent the formation of disulfide linkages. Due to the tendency of the protein to form disulfide-linked dimers, the spectroscopic studies in this work have been performed in the presence of DTT.

Intrinsic Fluorescence Spectra. Calbindin D_{28k} contains two Trp residues located at homologous positions in EF-hands 1 and 3 (in the first helix). The human recombinant, chicken intestinal, and bovine brain calbindin D_{28k} displayed similar changes in intrinsic fluorescence spectra after addition/removal of Ca^{2+}or alteration of the pH. Thus, the Trp fluorescence spectra of the apo and Ca^{2+}-loaded forms displayed emission maxima at 335 nm, indicating that the two Trp residues are not well exposed to water in either the apo or Ca^{2+}-bound state (Figure 5). The Ca^{2+}-loaded form, however, displayed a higher emission maximum than the apo

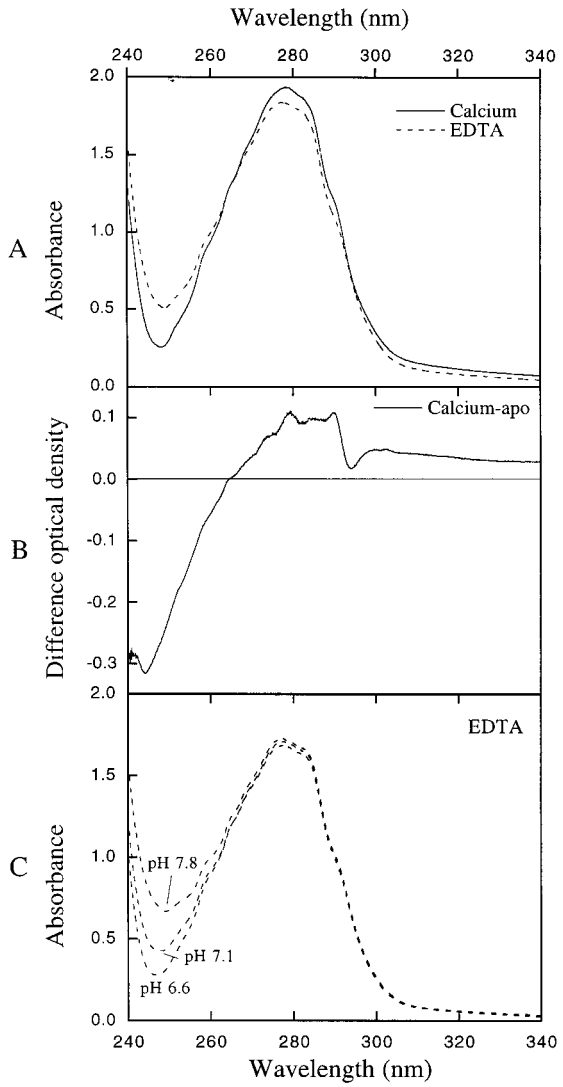

FIGURE 6: UV absorbance spectroscopy of calbindin D_{28k} in the presence or absence of Ca^{2+}. (A) UV absorbance spectrum of 68 μM human recombinant calbindin D_{28k}, in 10 mM DTT, 0.15 M KCl, 0.125 mM EDTA, and 2 mM Tris, pH 7.3 (apo calbindin D_{28k}; ---) at room temperature. $CaCl_2$ (1.25 mM) was then added to the same solution (Ca^{2+}-calbindin D_{28k}; —). (B) UV absorbance difference spectrum. The spectrum obtained in the presence of EDTA was subtracted from that obtained in the presence of Ca^{2+}. (C) UV absorbance spectrum for 63 μM human recombinant calbindin D_{28k}, in 10 mM DTT, 0.15 M KCl, 0.125 mM EDTA, and 2 mM Tris (apo calbindin D_{28k}; ---) at pH 6.6, 7.1, and 7.8.

form (by a factor of 1.3−1.1 depending on the species studied). Addition of excess EDTA returned the emission intensity to the initial value. The results indicate a reversible change of the fluorescence quenching of the two Trp residues after binding/dissociation of Ca^{2+}. Trp fluorescence spectra of the apo and Ca^{2+}-loaded forms were also recorded at different pH values (Figure 5). When the pH was changed from 6.6−7.8, the fluorescence intensity at 335 nm of Ca^{2+}-calbindin D_{28k} decreased slightly (∼2%) and the fluorescence intensity of apo calbindin D_{28k} increased by ca. 9%. The spectral changes were reversible, suggesting that the underlying structural changes are bidirectional.

UV Absorbance Spectroscopy. The UV absorbance spectrum of calbindin D_{28k} in the apo form displayed a maximum at 279.7 nm, which was shifted to 277.4 nm when Ca^{2+} was added (Figure 6A). The UV difference spectrum induced by

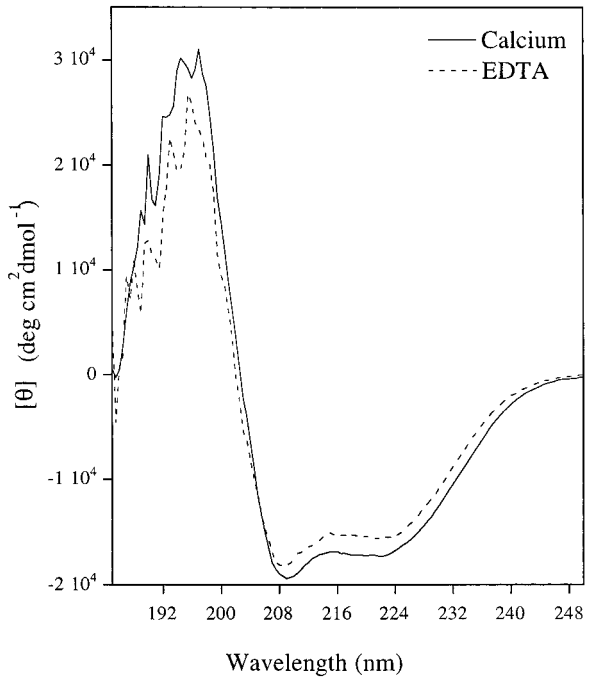

FIGURE 7: Far-UV circular dichroism spectra of calbindin D_{28k} The far-UV CD spectrum (185−250 nm) at 25 °C of 9 μM human recombinant calbindin D_{28k}, in 1 mM DTT and 2 mM Tris, pH 7.5, with 0.125 mM EDTA (apo calbindin D_{28k}; ---), or 1.25 mM $CaCl_2$ (Ca^{2+}-calbindin D_{28k}; —).

Ca^{2+} binding showed a negative absorbance at 240−265 nm and a positive absorbance between 265 and 320 nm, indicating that a conformational change has occurred in the local environment around aromatic residues upon Ca^{2+} binding (Figure 6B). The peaks at 280, 284, 290, and 294 nm most likely reflect rearrangement in the Trp environment, although some of the 280 and 284 nm peaks as well as the 273 nm peak may result from effects on Tyr residues. The negative peak at 244 nm may reflect increased light scattering in the apo state or alternatively effects on Phe residues. Under the conditions used (2 mM Tris and 10 mM DTT, pH 7.5), the extinction coefficients at 280 nm were 2.8×10^4 M^{-1} cm^{-1} for Ca^{2+}-loaded calbindin D_{28k} and 2.6×10^4 M^{-1} cm^{-1} for Ca^{2+}-free calbindin D_{28k}. When the pH was changed stepwise from 6.6 to 7.8, an increase in absorbance below 270 nm was seen for both the apo and Ca^{2+} states (Figure 6C). Similar Ca^{2+}- and pH-dependent changes in the UV absorbance spectra were observed for both human recombinant and bovine brain calbindin D_{28k} .

Far-UV CD. The far-UV CD spectra of the apo and Ca^{2+} forms of calbindin D_{28k} (Figure 7) were indicative of an α-helical protein and Ca^{2+} binding induced a small (12%) increase in ellipticity at 222 nm. Similar changes have been described for many other EF-hand proteins. For example, calmodulin displays an increase in CD signal on Ca^{2+} binding (*35*), although the high-resolution structures of the Ca^{2+} and apo states reveal the same number of residues in helical conformation (*36*−*38*). The lower CD signal in the apo state may reflect a more fluctuating structure, rather than a loss in the number of helical residues (*39*). The far-UV CD spectra of calbindin D_{28k} remained quite similar in the pH range 6.5−8.5, indicating that the secondary structure content is not significantly altered in the pH range examined (not shown).

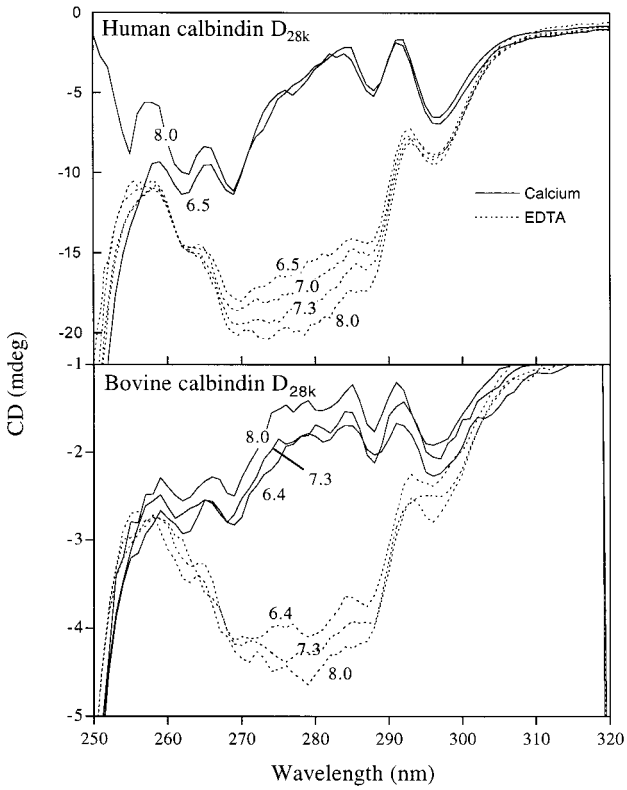

FIGURE 8: Near-UV circular dichroism spectra of calbindin D_{28k} The near-UV CD spectra (250−320 nm) were recorded at 25 °C for a solution of 68 μM human recombinant calbindin D_{28k} or 15 μM bovine brain calbindin D_{28k} in 10 mM DTT, 2 mM Tris, 0.125 mM EDTA (apo calbindin D_{28k}; ---). $CaCl_2$ (1.25 mM) was then added to the same solution (Ca^{2+}-calbindin D_{28k}; —). The pH of the solution was adjusted by addition of KOH or HCl as indicated in the figure.

Near-UV CD. The near-UV CD spectrum of calbindin D_{28k}, especially between 270 and 290 nm, was markedly altered by addition of Ca^{2+}, indicating a reorganization of the tertiary structure around aromatic residues (Figure 8). pH-Dependent spectral changes, reversible on a time scale of manual mixing, were readily seen (Figure 8). The pH-dependent spectral change was more pronounced in the Ca^{2+}-free protein. The CD signal decreased as a function of increasing $[H^+]$ or $[Ca^{2+}]$. This indicates that conformational changes affecting the local environment and/or rotational freedom of the aromatic residues occur both on Ca^{2+} binding and on pH changes. The Ca^{2+}- and pH-dependent changes in the near-UV CD spectra as described above were observed also for bovine brain calbindin D_{28k} (Figure 8), while the limited availability of calbindin D_{28k} purified from chicken intestine prevented us from performing a comparable analysis with this homologue.

Urea Denaturation of Apo Calbindin D_{28k} Followed by Circular Dichroism Spectroscopy and Fluorescence Spectroscopy. Urea-induced unfolding of calbindin D_{28k} was monitored by far-UV CD and Trp fluorescence. The Ca^{2+}-loaded form of the protein is only half denatured in 10 M urea at 90 °C (Berggård et al., unpublished results), suggesting that binding of Ca^{2+} greatly increases the stability toward unfolding of the protein. Hence, the stability measurements were performed in the presence of 1 mM EDTA. Measurements by far-UV CD and Trp fluorescence spectroscopy, respectively, yielded very similar values of the free energy of unfolding, $\Delta G_{NU}(H_2O)$, as well as the unfolding

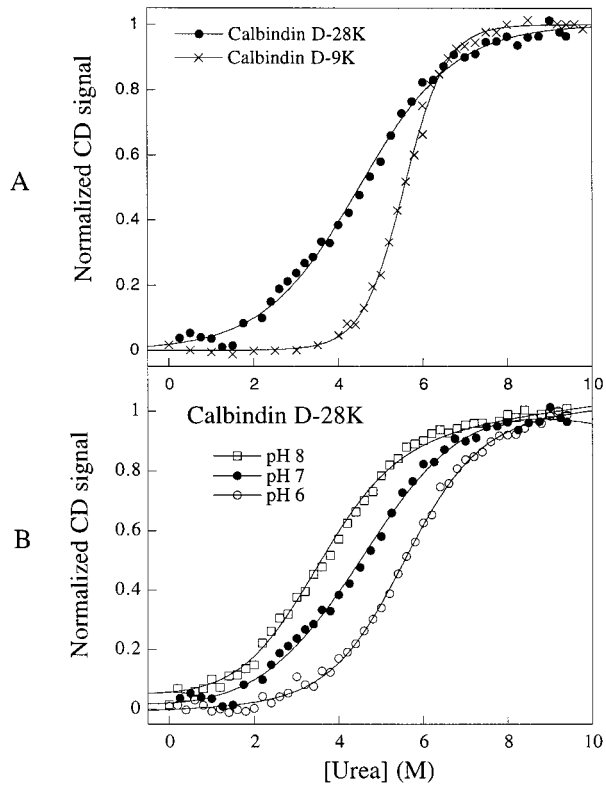

FIGURE 9: Urea-induced unfolding of calbindin D_{28k} and calbindin D_{9k}. Apparent fraction unfolded, F_{app}, is plotted as a function of urea concentration at 25 °C for (A) human recombinant calbindin D_{28k} (●) or bovine recombinant calbindin D_{9k} (×) at pH 7.0 and (B) for human recombinant calbindin D_{28k} at pH 8.0 (□), 7.0 (●) and 6.0 (○). The unfolding data for calbindin D_{9k} have been presented elsewhere (*41*). Denaturation parameters were obtained by fitting eq 3 directly to the CD data (ellipticity at 222 nm), and the data were then converted to F_{app} according to eq 5.

Table 1: Protein Stability, $\Delta G_{NU}(H_2O)$, of Calbindin D_{28k} at Different pHs

protein	pH	$\Delta G_{NU}(H_2O)$ (kJ mol^{-1})	m_{urea}[a] (kJ mol^{-1} M^{-1})	C_M[b] (M)
calbindin D_{28k}	6.0	14.7 ± 0.23	2.7 ± 0.04	5.4
calbindin D_{28k}	7.0	9.8 ± 0.23	2.2 ± 0.05	4.5
calbindin D_{28k}	8.0	8.3 ± 0.12	2.3 ± 0.02	3.6

[a] Linear denaturant dependence in the equation $\Delta G_{NU} = \Delta G_{NU}(H_2O) - m$[urea]. [b] Unfolding midpoint concentration.

transition midpoints. This indicates that both the secondary and the tertiary structure are disrupted in one concerted step. The results support a model in which all six EF hands are packed in a single domain, as suggested previously (*40*). To obtain information on the effect of the pH-dependent conformational change on stability, the ellipticity at 222 nm as a function of urea concentration was recorded at three different pHs (Figure 9B). The results show a clear dependence of the protein stability on pH, with the free energy of unfolding increasing by a factor of approximately 1.8 from pH 8 to 6 (see Table 1). Hence, the pH-dependent conformational change detected by other methods is sufficient also to affect protein stability. At all pHs, the $\Delta G_{NU}(H_2O)$ was relatively low, between 14.7 (at pH 6.0) and 8.3 kJ mol^{-1} (at pH 8.0), for calbindin D_{28k}. As a comparison, $\Delta G_{NU}(H_2O)$ for apo calbindin D_{9k} at pH 7.0 is significantly higher, 27.4 ± 1.3 (*41*) (Figure 9A). Thus, when the Ca^{2+}-free form is considered, calbindin D_{28k} does not rank among the most stable Ca^{2+}-binding proteins. The linear dependency of the free energy toward unfolding on the denaturant concentration, m_{urea}, reflects the cooperativity of the unfolding reaction. The low value of m_{urea} (2.2−2.7 kJ mol^{-1} M^{-1}) indicates that unfolding of calbindin D_{28k} involves a low degree of cooperativity. Alternatively, an apparent low m_{urea} could also indicate that the protein contains multiple domains that unfold independently (see Discussion).

DISCUSSION

Both the Ca^{2+}-Loaded and Ca^{2+}-Free Forms of Calbindin D_{28k} Have Exposed Hydrophobic Surfaces. Ca^{2+} sensors, such as calmodulin and troponin C, undergo a Ca^{2+}-induced conformational change, which exposes hydrophobic surfaces designed to interact with target proteins. In this study we have investigated possible sensor functions of calbindin D_{28k} using both recombinant human calbindin D_{28k} and protein purified from chicken intestine or bovine brain. Ca^{2+}-sensors such as calmodulin normally expose hydrophobic surfaces only in the Ca^{2+}-loaded state (Figure 1). This reflects their ability to function as Ca^{2+}-dependent on/off switches. In contrast, a typical Ca^{2+}-buffer/transport protein like calbindin D_{9k} does not expose hydrophobic patches under any conditions (Figure 1). The results in this study indicate that hydrophobic regions are exposed on the surface of calbindin D_{28k} in both the Ca^{2+}-free and Ca^{2+}-loaded states. Thus, in this respect calbindin D_{28k} does not behave like a traditional Ca^{2+} sensor but especially not like a typical Ca^{2+} buffer. A protein designed only to bind Ca^{2+} with high affinity should not benefit from having exposed hydrophobic surfaces. Exposure of hydrophobic surfaces is thermodynamically unfavorable, and therefore we suggest that calbindin D_{28k} may interact with as-yet-unknown target molecules. The existence of interactions between calbindin D_{28k} and membrane components of chick intestinal brush border membranes (*42*) and cerebellar microsomal fractions (*43*) have been described, implying that calbindin D_{28k} might have physiological target molecules associated with membranes.

Ca^{2+}-Induced Conformational Changes in Calbindin D_{28k}. Calretinin, a six-EF-hand protein that is highly homologous to calbindin D_{28k} (58% sequence identity), has been shown to undergo Ca^{2+}-induced conformational changes detected, for example, by spectroscopic methods and limited proteolysis (*44*−*46*). It has therefore been suggested that calretinin belongs to the sensor class of Ca^{2+}-binding proteins. Calbindin D_{28k} is still regarded mainly as a Ca^{2+}-buffering protein. Near-UV CD, intrinsic fluorescence measurements, and UV absorbance spectroscopy presented unequivocal evidence of Ca^{2+}-induced conformational changes in calbindin D_{28k}. The Ca^{2+}-induced changes in the amount of *exposed hydrophobic surface* of calbindin D_{28k} were, however, considerably less pronounced than that in calmodulin. This indicates that the protein does not operate in a similar manner as calmodulin but does not exclude that calbindin D_{28k} interacts with targets in a Ca^{2+}-dependent manner. The Ca^{2+} state is more stable than the apo state (see below). A higher level of structural definition of a potential binding site may promote a higher affinity for the target in the Ca^{2+} state. It is also possible that the protein uses several hydrophobic patches to bind to targets and that some of these are exposed in the presence of Ca^{2+}, whereas some are exposed in the absence of Ca^{2+}. Such a mechanism could

explain the Ca^{2+}-dependent conformational changes detected by spectroscopic methods as well as the fact that calbindin D_{28k} seems to adopt an "open" conformation in both the Ca^{2+} and apo state.

Calbindin D_{28k} Undergoes a Proton-Induced Conformational Change. The intracellular pH is usually around 7.1−7.2. However, changes in intracellular pH between 7.4 and 6.8 are common neuronal events (*47*), and the pH may occasionally drop down to 6.6 during cerebral acidosis (*48*). Structural changes of calbindin D_{28k} in the pH range between 6.5 and 8 were apparent in both human recombinant, bovine brain, and chicken intestinal calbindin D_{28k}. The far-UV CD spectrum of calbindin D_{28k} was not significantly altered in the pH range examined, suggesting that the secondary structure of the protein is intact in the physiological pH range. Hence, the side-chain interactions that characterize the tertiary structure of the native protein are most likely affected by small changes in pH. Protonation of critical side chain(s) could be assumed to underlie the acid-induced structural change in calbindin D_{28k}. Possible candidates are the terminal amino group, the imidazole group of His residues, or upshifted Asp or Glu carboxylates. The excess negative charge on calbindin D_{28k} may yield upshifted pK_a values of acidic residues to the 6−6.5 range, as was recently found for calbindin D_{9k} (unpublished experiments). The H^+-induced conformational change was shown to take place mostly in the N-terminal half of the molecule (residues 1−132, EF-hand 1−3), which contains all four His residues in the human and bovine protein. Three of these residues are conserved in the chicken homologue. Proton-induced conformational changes in the same pH range as described here have also been reported for calmodulin-dependent enzymes (*34*). In this case, H^+ was suggested to expose the calmodulin-binding domain on the target enzyme (*49*). Similarly, it is possible that the conformational change of calbindin D_{28k} in response to H^+ reflects exposure of a binding domain that may influence yet-unknown regulatory functions of the protein.

Stability of Calbindin D_{28k} Increases in Response to Acidic pH. The stability of the protein was increased as a response to increased H^+ concentration. This may be due to protonation of side chains and consequently a reduction in net negative charge of the protein. Like many other EF-hand proteins, calbindin D_{28k} has a high proportion (33%) of charged amino acid residues, 48 Asp + Glu and 31 Arg + Lys. Substituting negatively charged solvent-exposed residues (Glu and Asp) with uncharged side-chain amide analogues (Gln and Asn) in the overall negatively charged calbindin D_{9k} results in an increased stability toward unfolding (*50*). Hence, electrostatic repulsion between like charges on the surface of a folded protein decreases protein stability. Another factor that could contribute to the observed stability effects is the formation of hydrogen bond(s) on protonation. Such a mechanism could explain the pH-induced conformational shift as well as the increased stability of the protein at lower pHs.

Calbindin D_{28k} Unfolds in a Single Step as One Domain with Low Cooperativity. The change in secondary and tertiary structure of calbindin D_{28k} as a function of urea concentration was followed by CD spectroscopy and tryptophan fluorescence spectroscopy. The Ca^{2+}-loaded form of calbindin D_{28k} does not unfold even in the presence of 10 M urea (Berggård et al., manuscript in preparation), suggesting that the stability of the protein is greatly increased after binding of Ca^{2+}. Previous studies have shown that the Ca^{2+} forms of EF-hand proteins are often exceptionally stable and impossible to completely unfold with urea (see, for example, ref *51*). The linear dependencies of the free energy toward unfolding, $\Delta G_{NU}(H_2O)$, on the denaturant concentration, m_{urea}, was relatively low for Ca^{2+}-free calbindin D_{28k}, which sometimes is taken to indicate that the protein has multiple domains that unfold separately. Calmodulin has two domains consisting of two EF-hands each and a low m_{urea} value (*35*), similar to that observed here for calbindin D_{28k}. Recent data, however, suggest that all six EF-hands are part of a single globular domain (*40*). Moreover, the secondary and tertiary structures appear to unfold simultaneously, suggesting a two-step mechanism with no intermediates. Consequently, the presence of multiple domains in calbindin D_{28k} is not a likely explanation for the low m_{urea} observed here for calbindin D_{28k}. A more probable explanation is that calbindin D_{28k} unfolds in a single step with low cooperativity.

CONCLUSION

This study provides clear evidence that the structures of the Ca^{2+} and apo forms of calbindin D_{28k} are different. The results also indicate that calbindin D_{28k} displays some properties that are unusual in typical Ca^{2+}-sensors: The protein has exposed hydrophobic surfaces in both the apo and Ca^{2+} states, and it responds to H^+ in the neutral pH range with an increased stability and a conformational shift. It is unlikely that a protein designed only to bind Ca^{2+} for the purpose of lowering cytosolic Ca^{2+} concentration would have all these properties. On the basis of the results in this study, we propose that calbindin D_{28k} may interact with target molecules in a regulated manner. Work is in progress in our laboratory to purify and identify such targets.

ACKNOWLEDGMENT

We are thankful to Dr. Karin Julenius, Lund, University, for providing data of the urea denaturation of calbindin D_{9k} and to Professor Karin Åkerfeldt, Haverford College, for stimulating discussions.

REFERENCES

1. Kretsinger, R. H., and Nockolds, C. E. (1973) *J. Biol. Chem. 248*, 3313−26.
2. Nelson, M. R., and Chazin, W. J. (1998) *Biometals 11*, 297−318.
3. Wasserman, R. H., Taylor, A. N., and Kallfelz, F. A. (1966) *Am. J. Physiol. 211*, 419−23.
4. Hermsdorf, C. L., and Bronner, F. (1975) *Biochim. Biophys. Acta 379*, 553−61.
5. Christakos, S., Friedlander, E. J., Frandsen, B. R., and Norman, A. W. (1979) *Endocrinology 104*, 1495−503.
6. Fortin, M., and Parent, A. (1997) *J. Chem. Neuroanat. 14*, 51−61.
7. Mikkonen, M., Soininen, H., and Pitkanen, A. (1997) *J. Comp. Neurol. 388*, 64−88.
8. McDonald, T. J., Li, C., and Wasserman, R. H. (1995) *Brain Res. 675*, 303−15.
9. Friauf, E. (1994) *J. Comp. Neurol. 349*, 193−211.
10. Bastianelli, E., and Pochet, R. (1994) *Neurosci. Lett. 169*, 223−6.
11. Arai, R., Jacobowitz, D. M., and Deura, S. (1994) *Brain Res. Bull. 33*, 595−614.
12. Seress, L., Leranth, C., and Frotscher, M. (1994) *J. Hirnforsch. 35*, 473−86.

13. Christakos, S., Gabrielides, C., and Rhoten, W. B. (1989) *Endocr. Rev. 10*, 3−26.
14. Bredderman, P. J., and Wasserman, R. H. (1974) *Biochemistry 13*, 1687−94.
15. Leathers, V. L., Linse, S., Forsen, S., and Norman, A. W. (1990) *J. Biol. Chem. 265*, 9838−41.
16. Gross, M. D., Nelsestuen, G. L., and Kumar, R. (1987) *J. Biol. Chem. 262*, 6539−45.
17. Cheung, W. T., Richards, D. E., and Rogers, J. H. (1993) *Eur. J. Biochem. 215*, 401−10.
18. Veenstra, T. D., Johnson, K. L., Tomlinson, A. J., Naylor, S., and Kumar, R. (1997) *Biochemistry 36*, 3535−42.
19. Åkerfeldt, K. S., Coyne, A. N., Wilk, R. R., Thulin, E., and Linse, S. (1996) *Biochemistry 35*, 3662−9.
20. Airaksinen, M. S., Eilers, J., Garaschuk, O., Thoenen, H., Konnerth, A., and Meyer, M. (1997) *Proc. Natl. Acad. Sci. U.S.A. 94*, 1488−93.
21. Roberts, W. M. (1994) *J. Neurosci. 14*, 3246−62.
22. Chard, P. S., Bleakman, D., Christakos, S., Fullmer, C. S., and Miller, R. J. (1993) *J. Physiol. (London) 472*, 341−57.
23. Mattson, M. P., Rychlik, B., Chu, C., and Christakos, S. (1991) *Neuron 6*, 41−51.
24. Sloviter, R. S., Sollas, A. L., Barbaro, N. M., and Laxer, K. D. (1991) *J. Comp. Neurol. 308*, 381−96.
25. Sloviter, R. S. (1989) *J. Comp. Neurol. 280*, 183−96.
26. Feher, J. J., Fullmer, C. S., and Wasserman, R. H. (1992) *Am. J. Physiol. 262*, C517−26.
27. Ikura, M. (1996) *Trends Biochem. Sci. 21*, 14−7.
28. Skelton, N. J., Kordel, J., Akke, M., Forsen, S., and Chazin, W. J. (1994) *Nat. Struct. Biol. 1*, 239−45.
29. Thulin, E., and Linse, S. (1999) *Protein Expression Purif. 15*, 265−70.
30. Friedlander, E. J., and Norman, A. W. (1980) *Methods Enzymol. 67*, 504−8.
31. Waltersson, Y., Linse, S., Brodin, P., and Grundstrom, T. (1993) *Biochemistry 32*, 7866−71.
32. Johansson, C., Brodin, P., Grundstrom, T., Thulin, E., Forsen, S., and Drakenberg, T. (1990) *Eur. J. Biochem. 187*, 455−60.
33. Santoro, M. M., and Bolen, D. W. (1988) *Biochemistry 27*, 8063−8.
34. Huang, S., Carlson, G. M., and Cheung, W. Y. (1994) *J. Biol. Chem. 269*, 7631−8.
35. Martin, S. R., and Bayley, P. M. (1986) *Biochem. J. 238*, 485−90.
36. Finn, B. E., Evenas, J., Drakenberg, T., Waltho, J. P., Thulin, E., and Forsen, S. (1995) *Nat. Struct. Biol. 2*, 777−83.
37. Kuboniwa, H., Tjandra, N., Grzesiek, S., Ren, H., Klee, C. B., and Bax, A. (1995) *Nat. Struct. Biol. 2*, 768−76.
38. Zhang, M., Tanaka, T., and Ikura, M. (1995) *Nat. Struct. Biol. 2*, 758−67.
39. Hirst, J. D., and Brooks, C. L., 3rd (1994) *J. Mol. Biol. 243*, 173−8.
40. Linse, S., Thulin, E., Gifford, L. K., Radzewsky, D., Hagan, J., Wilk, R. R., and Akerfeldt, K. S. (1997) *Protein Sci. 6*, 2385−96.
41. Julenius, K., Thulin, E., Linse, S., and Finn, B. E. (1998) *Biochemistry 37*, 8915−25.
42. Leathers, V. L., and Norman, A. W. (1993) *J. Cell. Biochem. 52*, 243−52.
43. Winsky, L., and Kuznicki, J. (1995) *J. Neurochem. 65*, 381−8.
44. Schwaller, B., Durussel, I., Jermann, D., Herrmann, B., and Cox, J. A. (1997) *J. Biol. Chem. 272*, 29663−71.
45. Kuznicki, J., Wang, T. L., Martin, B. M., Winsky, L., and Jacobowitz, D. M. (1995) *Biochem. J. 308*, 607−12.
46. Kuznicki, J., Strauss, K. I., and Jacobowitz, D. M. (1995) *Biochemistry 34*, 15389−94.
47. Kiss, L., and Korn, S. J. (1999) *J. Neurophysiol. 81*, 1839−47.
48. Yates, C. M., Butterworth, J., Tennant, M. C., and Gordon, A. (1990) *J. Neurochem. 55*, 1624−30.
49. Huang, S., and Cheung, W. Y. (1994) *J. Biol. Chem. 269*, 22067−74.
50. Akke, M., and Forsen, S. (1990) *Proteins: Struct., Funct., Genet. 8*, 23−9.
51. Wendt, B., Hofmann, T., Martin, S. R., Bayley, P., Brodin, P., Grundstrom, T., Thulin, E., Linse, S., and Forsen, S. (1988) *Eur. J. Biochem. 175*, 439−45.

BI992394G